VIRTUAL SENSORS IN ACTIVE NOISE CONTROL

This paper was awarded the
2000 PRESIDENT'S PRIZE.
This prize established in 1990 by the Australian Acoustical Society, is awarded to the best technical paper presented at the Australian Acoustical Society Conference by a member of the Society.

Colin D. Kestell, Colin H. Hansen and Ben S. Cazzolato
Department of Mechanical Engineering,
University of Adelaide SA 5005, Australia

ABSTRACT: Traditional active noise control systems achieve the greatest noise reduction at the locations of the error sensor(s). In many cases it is desirable to be able to achieve the maximum noise reduction remote from an error sensor. One way of doing this is to measure the transfer function between the desired location of maximum reduction and the error sensor and incorporate it in the control algorithm. The disadvantage of this method is that it is not robust to changes in the acoustic environment. Another method relies on using two or more microphones to estimate the sound level at a remote location using forward prediction. This method results in a lower performance but it can be adapted to changes in the acoustic environment as well as to changes in the location of the desired pressure minimum. This paper will report on a study that compares the relative merits of various forward prediction method in various situations. These commence with a free field environment (to introduce the concept) and then progress to a more practical application of an aircraft cabin. Single and multiple control sources will be considered as will sound pressure sensing and energy density sensing.

1. INTRODUCTION

Active noise control in modally dense and highly damped enclosures can result in small zones of attenuation that are centralised around the error sensors. In fact, an observer located close to a single acoustic pressure error sensor may not perceive any improvement in noise reduction as a result of active noise control, even though the error sensor may indicate that a significant reduction has been achieved. Consequently, research has recently been focused on finding alternative cost functions that results in a broader region of control that is sufficiently large to envelope the observer. Energy density is known to be more spatially uniform than squared acoustic pressure and can result in larger regions of attenuation when it is used as an active noise control cost function (Sommerfeldt and Parkins (1994)). However, for a multi-channel control system, the maximum attenuation in pressure is still likely to occur at the sensor location and the size of the zone of local control is inversely proportional to frequency (Cazzolato (1999)). The volume of the control region also tends to increase at the expense of reduced attenuation. An alternative to increasing the size of the control zone is to minimise the cost function at the observer rather than at the error sensor location by "virtual sensing", a concept first introduced by Garcia-Bonito *et al.* (1996). Their method was based on measuring the acoustic pressure transfer function between a permanently placed remote microphone and a microphone temporarily located at the observer location. With the temporary microphone subsequently removed, the signal from the permanent microphone was modified with the transfer function to create a *"virtual microphone"* at the observer location. However, any significant observer movement or environmental change within the vicinity of the sensors alter the transfer function and result in an error in the estimate of the acoustic pressure at the observer location. Kestell *et al.* (2000, 2001) introduced *"forward difference prediction virtual sensors"* which use multiple sensors to estimate a trend in the acoustic field and predict (via extrapolation) the cost function at the observer location. They have demonstrated various strategies of error sensing that not only shift the zone of attenuated noise towards an observer but combine the benefits of "virtual sensing" and energy density minimisation. This paper shows a summary of the theory, introduces the concept with an idealised free field example and shows how the virtual sensors perform in an aircraft cabin.

2. THEORY

With reference to figure 1, four *"forward difference prediction virtual sensors"* algorithms are summarised as follows:

1. Two microphone, first-order virtual micro-phone:

$$p_v \quad \frac{(p_2 \quad p_1)}{2h} x + p_2 \tag{1}$$

2. Three microphone, second-order virtual micro-phone:

$$p_x \quad \frac{x(x+h)}{2h^2} p \; + \; \frac{x(x+2h)}{h^2} p_2 + \frac{(x+2h)(x+h)}{2h^2} p_3 \tag{2}$$

3. Two microphone, first-order virtual energy density sensor:

$$E_{D_x} \quad \frac{}{4\rho c^2} \left| \left(+ \frac{x}{2h} \right)^2 p_2^2 \quad \frac{x}{h} \left(1 + \frac{x}{2h} \right) p \; p_2 \right.$$
$$\left. + \left(\frac{x}{2h} \right)^2 \rho_1^2 \quad \frac{1}{(2hk)^2} \left(p_2^2 \quad 2p_1 p_2 + p_1^2 \right) \right| \tag{3}$$

4. Three microphone second-order virtual energy density sensor:

$$E_{D_x} \quad \frac{}{4\rho c^2} \left| \left(\frac{x(x \; h)}{} p_1 + \frac{x(x \; 2h)}{h^2} p_2 \right.\right.$$
$$\left.\left. + \quad \frac{(x+2h)(x+h)}{2h^2} p_3 \right)^2 \right.$$
$$\frac{1}{k^2} \left(\frac{2x+h}{2h^2} \; p_1 \quad \frac{2x+2h}{h^2} \; p_2 + \frac{2x+3h}{2h^2} \; p_3 \right) \tag{4}$$

Where x is the distance between the observer and the nearest sensor, h (25mm) is the transducer separation distance, p_1, p_2 and p_3 are the measured pressures, p_x is the pressure at the observer location and E_{Dx} is the time averaged energy density at the observer location.

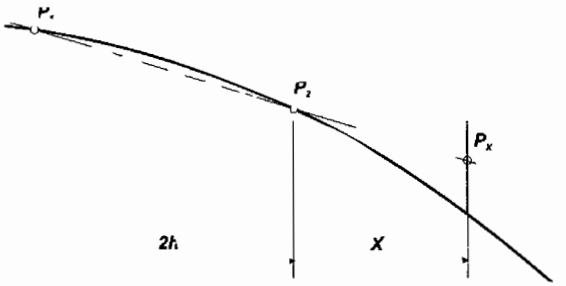

(a) First-order

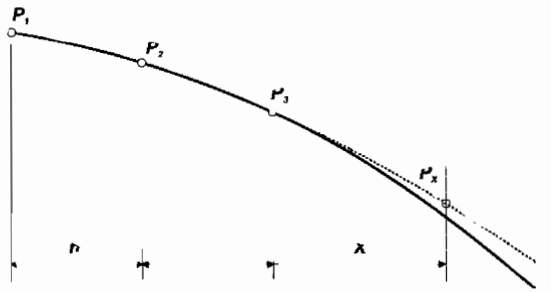

(b) Second order

Figure 1: Forward difference extrapolation

3. METHOD

The zone of local control around a "virtual energy density sensor" and a "virtual microphone" is compared with that achieved when using an actual energy density sensor and a single microphone. To introduce the concept, the analysis commences with a free field approximation in an anechoic chamber (figure 2) and then progresses to the more practical application of an aircraft cabin (figure 3).

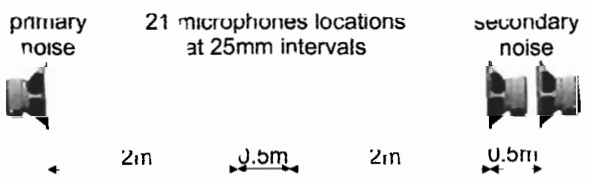

Figure 2: Schematic representation of the experimental configuration in an anechoic chamber.

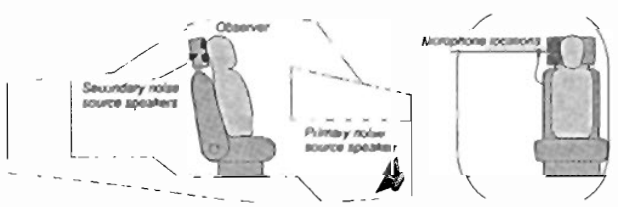

Figure 3: The speaker and microphone locations in the aircraft cabin.

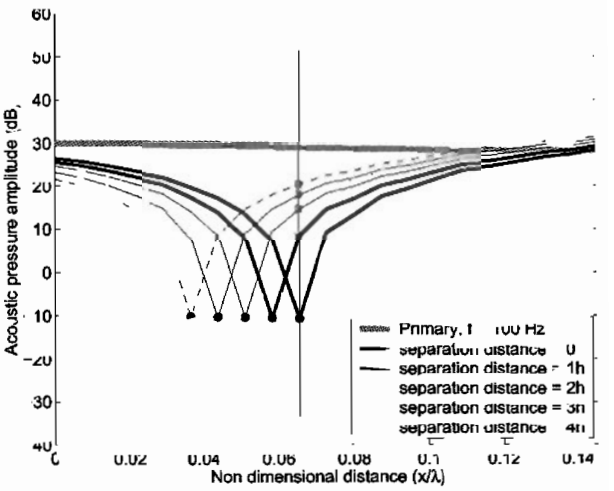

(a) Control via one microphone

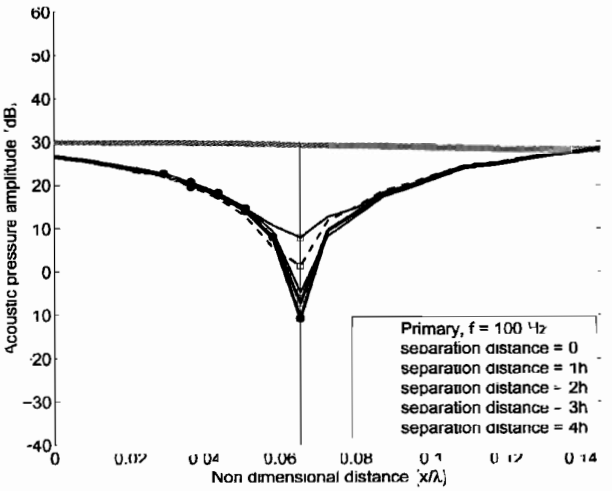

(b) A first-order virtual microphone

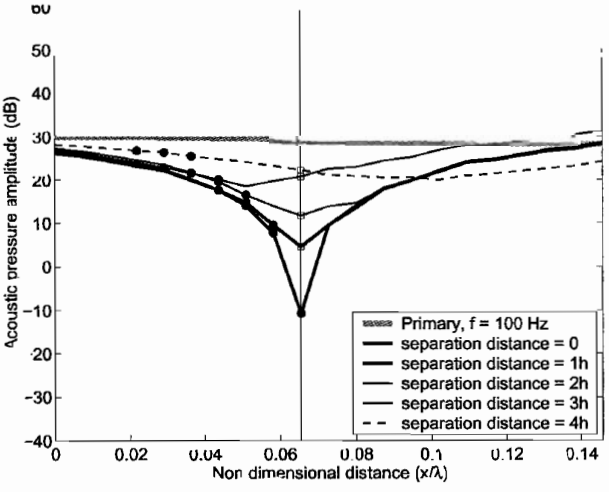

(c) A second-order virtual microphone

Figure 4: A 100 Hz primary sound source in an anechoic chamber controlled via one control source. The actual sensors are marked with a circle and the observer location by a vertical line.

In each example the primary noise was generated using a single acoustic source, the secondary (cancelling) noise was generated from either one or two control sources and the controlled sound field was analysed along a 0.5 m length at 25 mm increments. Minimising pressure at a single location only requires one control source, but Cazzolato (1999) showed that two control sources are required to effectively minimise energy density in one dimension. With two control sources, using a *first-order virtual energy density sensor* is identical to simply minimising energy density at the physical sensor location or acoustic pressure at two microphone locations (Kestell *et al.* (2000,2001)). This is because in a two sensor system the energy density estimate at the observer is a linear combination of the pressure and pressure gradient at the sensors. Therefore if these are zero at the sensors it follows that the estimated energy density will also be zero. Therefore, in the examples that follow, the use of a single control source is limited to observing the performance of a single microphone, a *first-order virtual microphone* and a *second-order virtual microphone*. Two control sources are used to observe energy density minimisation directly at the sensors and at the observer location with a *second-order virtual energy density sensor*.

Figure 5: Prediction errors in the absence of short wavelength spatial pressure variations.

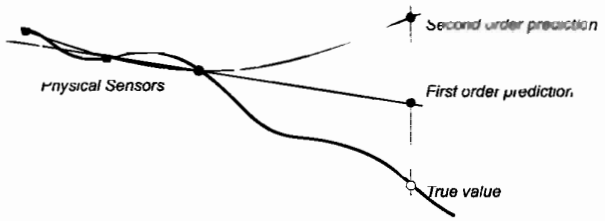

Figure 6: Prediction errors in the presence of short wavelength spatial pressure variations.

4. RESULTS

Control in an anechoic chamber

Figure 4 shows the results that are obtained when controlling a 100 Hz monotone in an anechoic chamber. The results in figure 4(a) show the level of control achieved when using a conventional pressure squared cost function, where the sensor is incre-mentally moved further from the observer location. The attenuation at the observer location is shown to reduces from 40 dB to 8 dB as the observer/sensor separation distance increases from *0h* to *4h* (100 mm). In figure 4(b) the control results for a *first-order virtual microphone* are shown. Since the algorithm adapts to an increasing separation distance, the attenuation only reduces to 22 dB when observer / sensor separation distance increases to 100 mm, demonstrating a practical advantage over the conventional remotely placed single microphone (figure 1). Figure 4(c) illustrates the performance of the theoretically more accurate *second-order virtual micro-phone* (refer to figure 1(b)), showing that its accuracy is adversely affected by small spatial pressure variations that are primarily due to reflections from the walls of the chamber (figures 5 and 6). In this example the *second-order virtual microphone* offers no practical advantage when compared to a single remotely placed microphone. Introducing a second control source allows the pressure to be independently controlled at two sensor locations and control of energy density either at the observer or the sensor location (Kestell *et al.* (2000,2001)). Energy density minimisation at the error sensor (or virtual first-order prediction at the observer location) is shown in figure 7(a).

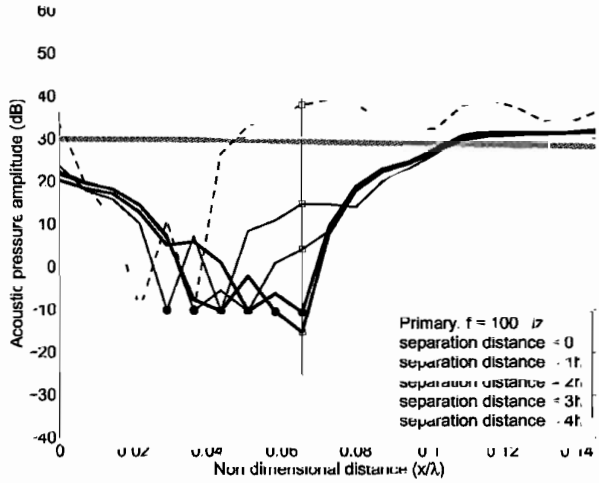

(a) Energy density control (and first-order virtual energy density control)

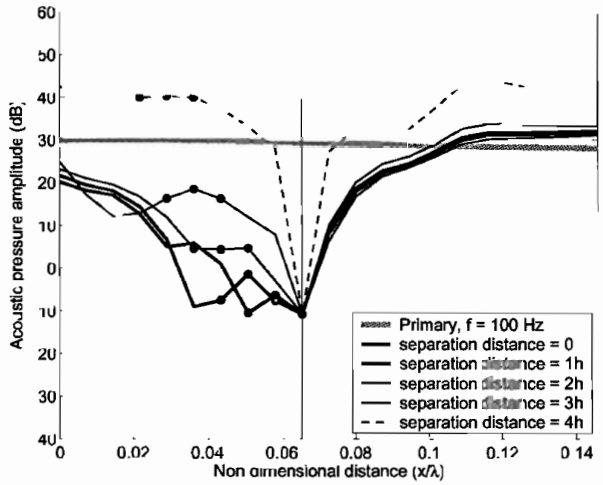

(b) Second-order virtual energy density control

Figure 7: A 100 Hz primary sound source in an anechoic chamber controlled via two control sources. The sensors are marked with a circle and the observer location by a vertical line.

Because of the second control source, this cost function produces a broader region of control (when compared to that obtained using a single error micro-phone and a single control source) and hence maintains an attenuation envelope around the observer location, until the sensors are moved to a separation distance of 100 mm (4h). At this observer/sensor separation distance the prediction inaccuracies result in a gain of 8 dB at the observer location. In figure 7(b) the performance of the *second-order virtual energy density sensor* is shown. The second-order prediction of the energy density cost function at the observer location is more rugged in the presence of small spatial pressure variations and maintains the maximum attenuation at the observer location within a broad and practically sized zone of attenuation.

An aircraft cabin

The results of actively controlling the primary noise between 50 Hz and 400 Hz with a single control source loudspeaker located in the head-rest of an aircraft cabin are shown in figure 8. Figure 8(a) shows how the uncontrolled noise levels at the observer location compare to the controlled noise levels using various error sensors, all located 100 mm from the observer.

The *second-order virtual microphone* is shown to be extremely sensitive to short wavelength noise and produces an erratic control profile across the entire frequency range. For a clearer comparison, the noise attenuation at the observer location, when using the first and second-order virtual microphone error sensors, is compared directly to that obtained using a single microphone error sensor (the 0 dB reference) in figure 8(b). It is shown, that for this single control source example, using a *first-order virtual microphone* results in an improved performance compared to that obtained using a remotely placed single microphone. Figure 9 shows the spatial variation of the uncontrolled primary noise and the controlled noise for each error sensor, at an example frequency selected from figure 8 (b), where using virtual microphones as error sensors improved the active noise control performance, compared to using a single microphone.

In the 254 Hz example it can be seen that when the error sensor is a single microphone, the high level of noise attenuation achieved at the sensor does not extend to encompass the observer 100 mm away with only 5 dB of attenuation achieved at the observer location. At the same observer location, the *second-order virtual microphone* results in 8 dB of attenuation and the *first-order virtual microphone* results in 20 dB.

Figure 10 illustrates the results of actively controlling the primary noise between 50 Hz and 400 Hz with two control sources located in the observer's head-rest. The spectra corresponding to the active noise control when using a single microphone, a *first-order virtual microphone* and a *second-order virtual microphone* are compared to the uncontrolled noise spectrum at the observer location, with sensors separated from the observer by 100 mm. Figure 10(a) shows that all of the control strategies considered here reduced the noise at the observer location across the entire frequency range of interest. In figure 10(b) the error sensing performance of both types of virtual energy density sensor are directly compared to the use of a single microphone (with one control source) in which control via the single microphone is the 0 dB reference.

Figure 11 shows that the zone of control increases with a *first-order virtual energy density sensor* (compared to using a *first-order virtual microphone*), but as a result of the second control source (and the independent control of pressure at two locations) and not the cost function. Figure 10(b) and figure 8(b) show that the *second-order virtual energy density sensor* shows a superior error sensing performance when compared to using all of the other error sensing methods. Figure 11 shows how the control zones compare in the spatial domain around the observer location at an example frequency of 233 Hz chosen from figure 10 (b). It is shown that the *second-order virtual energy density error sensor* not only results in the

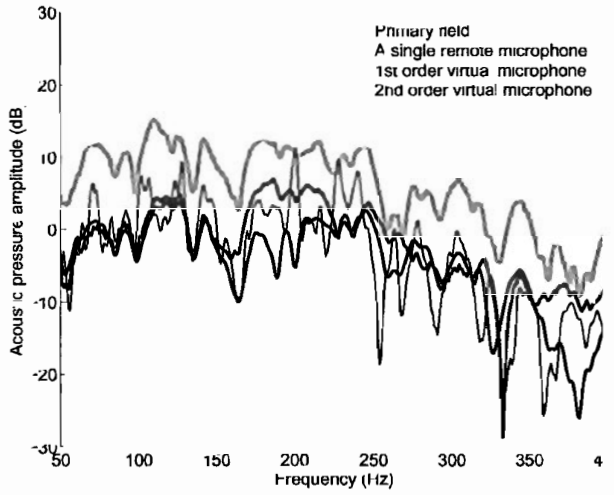

(a) The uncontrolled and controlled spectra for various error sensing strategies

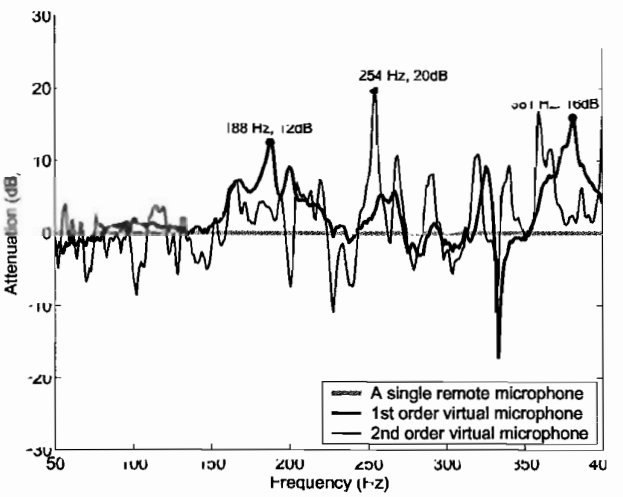

(b) The attenuation achieved with virtual microphones compared to a single microphone

Figure 8: ANC spectra at the observer location with one control source located in the observer's headrest. The sensors are located 4h (100mm) from the observer's ear.

highest noise attenuation at the observer location, but produces a broad zone (compared to a single microphone) of attenuated noise centered around the observer location.

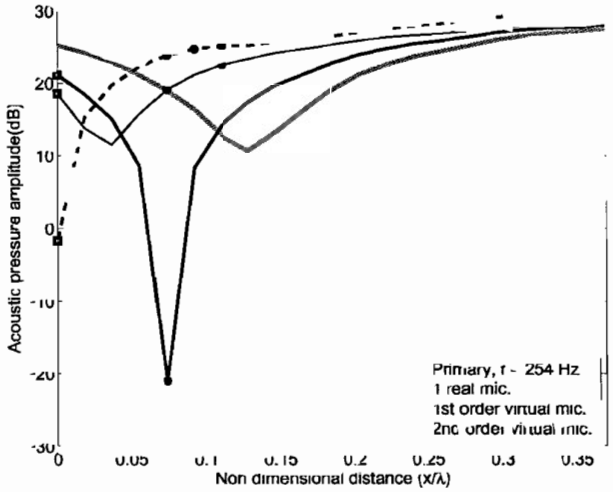

Figure 9: 254 Hz controlled using a single control source in the headrest. The sensors are marked with a circle and the observer location is at the far left hand side of each graph.

5. CONCLUSIONS

In the particular examples discussed in this paper, it has been demonstrated that the *first-order virtual microphone* (based on forward difference prediction) outperforms a conventional microphone (in terms of noise reduction at the observer location) for the same observer/sensor location separation distance. While the highest attenuation at the observer location should theoretically be achieved by using a *second-order virtual microphone*, the attenuation actually achieved was found to be very sensitive to short wavelength spatial pressure variations and seldom offered an advantage in practice to the use of a conventional microphone. It has also been shown that first-order prediction methods for energy density estimation at a remote location (the observer) offer no advantage to controlling energy density directly at the remote sensor. In terms of offering both a high level of attenuation and a broad control zone around the location of the observer, the *second-order virtual energy density sensor* produced the best results.

REFERENCES

1. B.S. Cazzolato. *Sensing systems for active control of sound transmission into cavities*. Ph.D. Thesis, The University of Adelaide, Adelaide, South Australia, April 1999.
2. J. Garcia-Bonito, S.J. Elliott, and C.C. Boucher, "A virtual microphone arrangement in a practical active headrest" *Proceedings of Inter-noise* 96, 1115-1120 (1996).
3. C.D. Kestell, B.S. Cazzolato, and C.H. Hansen, "Active noise control with virtual sensors in a long narrow duct" *Int. J. Acoust. & Vibn.*, 5(2):63-76, June (2000).
4. C.D. Kestell, B.S. Cazzolato, and C.H. Hansen, "Active noise control in a free field with virtual sensors." *J. Acoust. Soc. Am.*, 109(1):232-2436 (2001).
5. S.D. Sommerfeldt and J. Parkins "Active control of energy density in three dimensional enclosures" *J. Acous. Soc. Am.*, 95 (5):2989 (1994).

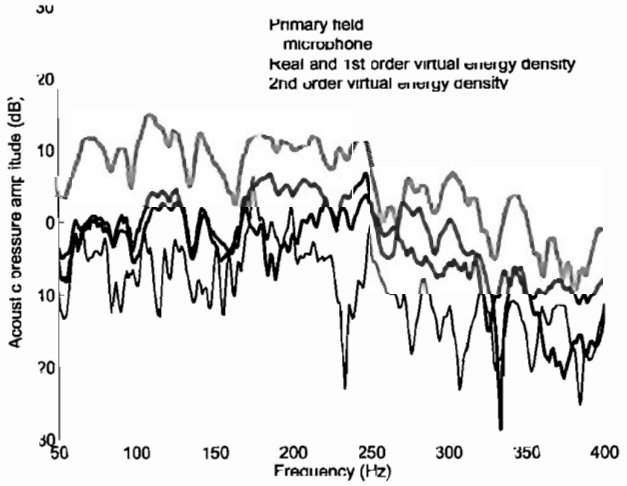

(a) The uncontrolled and controlled spectra for various error sensing strategies

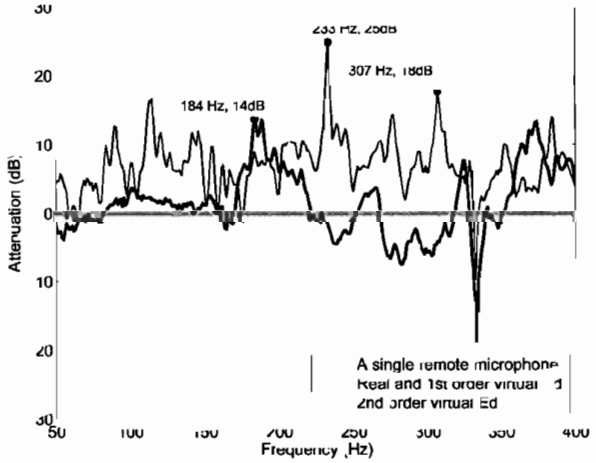

b) The attenuation achieved with virtual microphones compared to a single microphone

Figure 10: ANC spectrums at the observer location with two control sources both located in the observer's headrest. The physical sensors are located 4h (100mm) from the observer's ear.

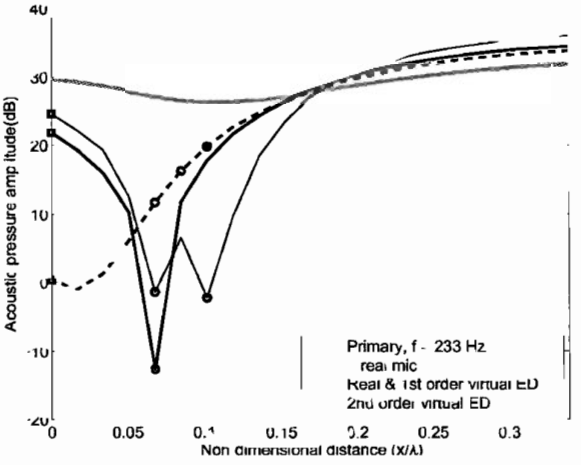

Figure 11: 233 Hz controlled using two control sources in the headrest. The sensors are marked with a circle and the observer location is at the far left hand side of each graph.